JOURNAL OF SOLID STATE CHEMISTRY **140,** 175–181 (1998)
ARTICLE NO. SC987839

Structure of $A_2Ge_4O_9$-Type Sodium Tetragermanate ($Na_2Ge_4O_9$) and Comparison with Other Alkali Germanate and Silicate Mixed Tetrahedral–Octahedral Framework Structures

M. E. Fleet[1] and S. Muthupari

Department of Earth Sciences, University of Western Ontario, London, Ontario N6A 5B7, Canada

Received December 4, 1997, in revised form March 16, 1998; accepted March 30, 1998

Long-standing uncertainty on the structure type of $Na_2Ge_4O_9$ has been resolved. Sodium tetragermanate has been grown by crystallization from a supercooled melt and its single-crystal X-ray structure has been determined ($R = 0.022$). Sodium tetragermanate is trigonal with $a = 11.3234(12)$, $c = 9.6817(9)$ Å, space group $P\bar{3}c1$, $Z = 6$, and $D_x = 4.451$ g cm^{-3}. The structure is comprised of a mixed tetrahedral–octahedral framework with three-membered [Ge_3O_9] rings of GeO_4 tetrahedra interconnected by isolated GeO_6 octahedra via shared corners and is $A_2Ge_4O_9$-type. Bond distances and angles for GeO_4 tetrahedra and GeO_6 octahedra are very similar to the corresponding values in the type structure of $K_2Ge_4O_9$, the two structures differing mainly in the accommodation of the smaller (medium–large-sized) Na cation, which is now in a 5 + 2 coordination. The structure–composition relationships of wadeite-type, $A_2Ge_4O_9$-type, and $Na_2Si_4O_9$-type structures of germanates and silicates depend largely on the *T*–O distance and the size of the monovalent cation. We confirm that sodium tetragermanate is a metastable phase at all pressures up to 2 kbar, the stable assemblage for the $Na_2Ge_4O_9$ composition being sodium enneagermanate ($Na_4Ge_9O_{20}$) plus a more sodic phase.

INTRODUCTION

The structures of alkali germanates ($mNa_2O.nGeO_2$) with $n > m$ tend to contain Ge in both octahedral and tetrahedral coordination and, therefore, are of particular interest as possible analogue structures for high-pressure silicates and silicate minerals in the Earth's mantle (1, 2). The large alkali–cation tetragermanates, tetrasilicates, and related compounds ($A_2BT_3O_9$, with A = K, Rb, Cs, and also Tl, Ag, B = Ge, Si, and also Ti, Sn, Zr, and T = Ge, Si) form mixed tetrahedral–octahedral framework structures in which three-membered [T_3O_9] rings of TO_4 tetrahedra are interconnected by isolated BO_6 octahedra via shared corners (3–6). Three structure types are known: wadeite ($K_2ZrSi_3O_9$, 3; space group $P6_3/m$; Fig. 1a), that is favored by silicates, $Tl_2TiGe_3O_9$, $Cs_2TiGe_3O_9$, and $Cs_2SnGe_3O_9$; $A_2Ge_4O_9$ (e.g., $K_2Ge_4O_9$, 4; space group $P\bar{3}c1$; Fig. 1b) that is favored by other germanates; and $Na_2Si_4O_9$ (7; space group $P2_1/n$). The unit cells of the two germanate structure types are related by $a \approx a(A_2Ge_4O_9) \approx a(\text{wadeite})\sqrt{3}$; $c \approx c(A_2Ge_4O_9) \approx c(\text{wadeite})$. In contrast, $Li_2Ge_4O_9$ and $LiNaGe_4O_9$ have a structure based on crenulated [Ge_3O_9]$_n$ chains of GeO_4 tetrahedra interconnected by GeO_6 octahedra (8, 9). Also, the structure of high-pressure $Na_2Si_4O_9$ has a nine-membered [Si_9O_{27}] ring of SiO_4 tetrahedra that is collapsed around and interconnected by SiO_6 octahedra (see Fig. 1c) (7).

The structure and phase stability of sodium tetragermanate ($Na_2Ge_4O_9$; a tetragermanate with a medium–large-sized alkali cation) have been debated extensively (4, 10–17) and remain controversial. Early work (10, 12) suggested that $Na_2Ge_4O_9$ was isostructural with $K_2Ge_4O_9$ and $Rb_2Ge_4O_9$ and that the tetragermanates of Na, K, Rb, and Tl were perhaps wadeite-type (18). Single-crystal camera and powder X-ray diffraction observations on $Na_2Ge_4O_9$ pointed to the space group $P6_3/m$ rather than $P\bar{3}c1$ (14). In their discussion of the $A_2Ge_4O_9$-type structure of $K_2Ge_4O_9$, Völlenkle and Wittmann (4) also assumed the space group of reference (14; $P6_3/m$) for $Na_2Ge_4O_9$, reporting that only tetragermanates of the large monovalent cations Rb, Tl, and Ag were isostructural with $K_2Ge_4O_9$. Subsequently, the wadeite structure was assigned to $Na_2Ge_4O_9$ (16) based on iterative refinement of positional parameters using 19 reflections of the powder X-ray diffraction pattern of reference (14).

Phase relations in the system Na_2O–GeO_2 at high GeO_2 content are complicated by the existence of two phases of similar composition; $Na_2Ge_4O_9$ and $Na_4Ge_9O_{20}$ (10–13, 15, 17; earlier work is reviewed in 15). The structure of sodium enneagermanate contains four-fold clusters of GeO_6 octahedra linked into columns by isolated GeO_4 tetrahedra

[1] To whom correspondence should be addressed. E-mail: mfleet@julian.uwo.ca.

0022-4596/98 $25.00

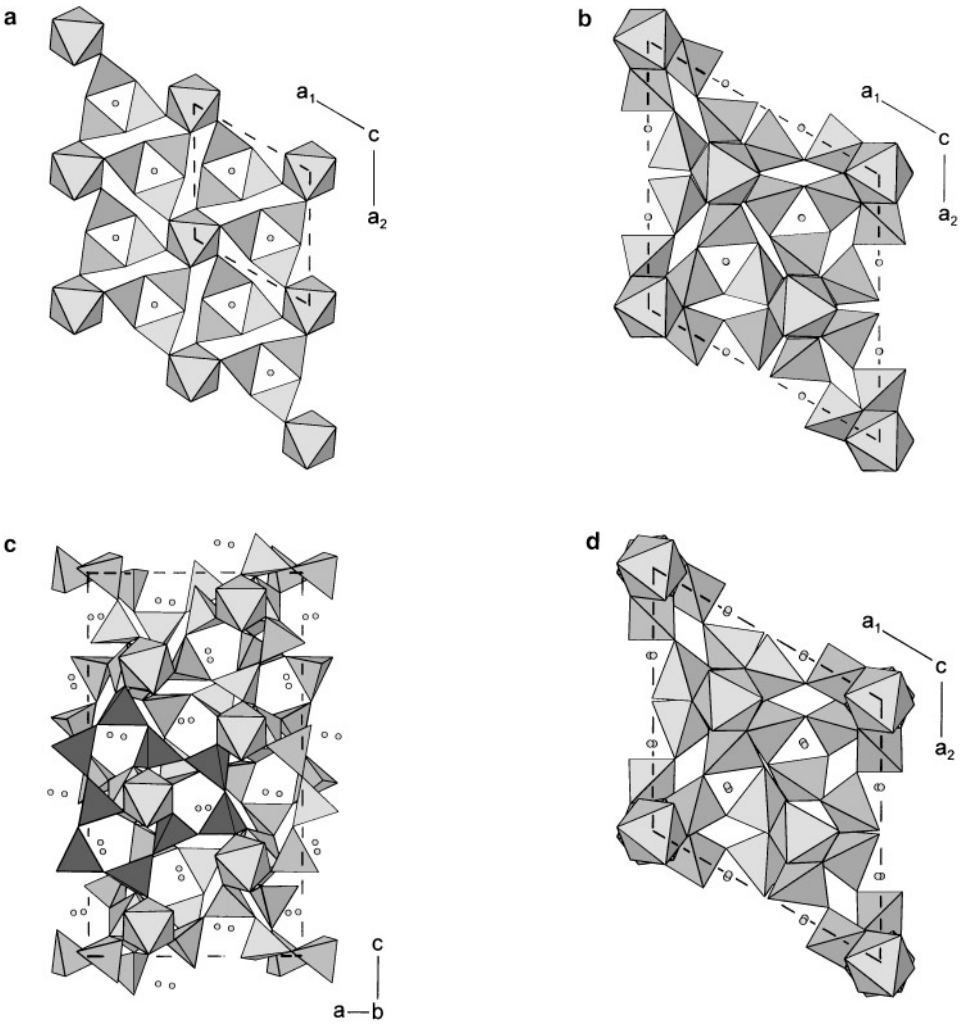

FIG. 1. Polyhedral representation of (a) wadeite-type structure of $K_2Si_4O_9$ (6), the GeO_6 octahedron is on unit-cell origin, (b) $A_2Ge_4O_9$-type structure of $K_2Ge_4O_9$ (4), the $Ge(1)O_6$ octahedron is on the origin, (c) $Na_2Si_4O_9$ structure (7), with a single nine-membered ring of nonequivalent tetrahedra highlighted, and (d) $A_2Ge_4O_9$-type structure of $Na_2Ge_4O_9$ (this study). Unit-cell outlines are indicated by broken lines.

and interconnected by spiral $[Ge_4O_{12}]_n$ chains of GeO_4 tetrahedra (19, 20). Sodium enneagermanate forms by hydrothermal reaction at 200°C and 12 bars (10, 21; see also 19), thermal decomposition of $Na_3HGe_7O_{16}(H_2O)_4$ in air at 600°C (10), crystallization of glass of composition $Na_2Ge_4O_9$ in air at all temperatures to the liquidus (10, 13), very slow cooling of melts in air to 600–700°C (12, 16), annealing $Na_2Ge_4O_9$ in air (10), crystallization using a sodium tungstate flux in air (20), and DTA experiments on sodium germanate glasses (17). It was earlier misidentified as a low-temperature polymorph of $Na_2Ge_4O_9$ (10–12). Sodium tetragermanate has been reported only from dry synthesis, e.g., slow cooling of melts of composition $Na_2Ge_4O_9$ in air to above 700°C (12, 16) and to an unspecified temperature (14), fusion of a stoichiometric mixture of GeO_2 and Na_2CO_3 at 900°C, and as an early product in the crystallization of GeO_2-rich glass (13, 17). Murty and Aguayo (13) questioned the existence of the tetragermanate phase, and Monnaye and Bouaziz (15) concluded that it is metastable at 1 bar.

We presently crystallize $Na_2Ge_4O_9$ from the melt, determine its crystal structure to be $A_2Ge_4O_9$-type, and further investigate the stability of this enigmatic phase.

EXPERIMENTAL PROCEDURES

Crystal Structure of Sodium Tetragermanate

Crystals of sodium tetragermanate ($Na_2Ge_4O_9$) were grown in a platinum dish from a 1.0 g mixture of high-purity GeO_2 and analytical grade Na_2CO_3. The mixture was melted at 1200°C and cooled at 100°C/h to 900°C, yielding

a supercooled melt, which was removed from the furnace for a few minutes then reheated to 900°C and cooled at 10°C/h to 800°C. The products consisted of large hexagonal prismatic crystals of $Na_2Ge_4O_9$ (up to 0.5 mm in diameter and 8 mm in length) and minor glass. The crystals were characterized as $Na_2Ge_4O_9$ by powder X-ray diffraction, using a Rigaku powder diffractometer system and Cu$K\alpha$ X-radiation, and petrographic microscopy (14). They were characterized as isostructural with $K_2Ge_4O_9$ using X-ray precession photography (space group $P\bar{3}c1$; 4).

Single-crystal measurements were made at room temperature and pressure with an Enraf–Nonius CAD-4F diffractometer and graphite-monochromatized Mo$K\alpha$ X-radiation ($\lambda = 0.71069$ Å). Structure refinements closely followed earlier procedures (7, 20) and started with the positional parameters for the $A_2Ge_4O_9$-type structure of $K_2Ge_4O_9$. Scattering factors for neutral atomic species and f', f'' were taken from (22). All computations were carried out with DATAP77 and LINEX77 (State University of New York at Buffalo). Results are summarized in Tables 1–4 and Figs. 1–3.

Sodium tetragermanate ($Na_2Ge_4O_9$) is trigonal with $a = 11.3234(12)$, $c = 9.6817(9)$ Å, $V = 1075.1$ (2) Å^3, space group $P\bar{3}c1$ (No. 165), $Z = 6$, and $D_x = 4.451$ g cm^{-3}. Three thousand and two reflections with indices $\pm h, \pm k, l$ and $2\theta \leq 45°$ and 3105 reflections with indices $h, k, \pm l$ and $45° < 2\theta \leq 75°$ were measured in the ω-scan mode. Transmission factors varied from 0.114 for 100 to 0.250 for $10, 4, \overline{11}$ (crystal volume $= 1.92 \times 10^{-3}$ mm^3, $\mu = 168.9$ cm^{-1}). There were 1897 unique reflections, with 925 considered unobserved on the basis of $I < 3\sigma(I)$. All reflections systematically absent in space group $P\bar{3}c1$ had zero intensity using $I < 3\sigma(I)$. Refinement in $P\bar{3}c1$ converged to $R = 0.0223$, $R_w = 0.0246$ (for reflections with $I \geq 3\sigma(I)$, $S = 0.421$, $g = 0.93(2) \times 10^{-4}$, $\Delta\rho = -0.72$ eÅ^{-3} near O(2) to 0.82 eÅ^{-3} near Ge(1)). All reflections were included in the refinement, but reflections with $I < 3\sigma(I)$ were given a low weight. The relatively low goodness-of-fit value (0.421) reflects crystal imperfection. Reflections with $I \geq 3\sigma(I)$ were assigned weights based on counting statistics. However, refinement with unit weights for these reflections resulted in the same structure (all parameters were unchanged within 1σ), and $R = 0.0223$, $R_w = 0.0254$, and $S = 1.380$.

Experiments on the Stability of Sodium Tetragermanate

Various experiments were made with melts and glass of $Na_2Ge_4O_9$ bulk composition prepared as above. Experiments in air were made with platinum dishes or crimped platinum capsules. Melts were prepared at 1100°C, and glasses were prepared by air quenching either 1100°C melts or supercooled melts. Melts were cooled from 1100°C to 900, 800, and 700°C at 1–30°C/h, with annealing times of 0–24 h. In one experiment, the supercooled melt was removed from the furnace at 800°C momentarily (~1 min) and then annealed for 2–3 min before quenching in air. Glass was annealed at 900°C for 30 min and 10 h, 800°C for 2 and 2.5 min and 15 h, 700°C for 168 h, and 500°C for 12 h, and cooled from 900 to 800°C at 10°C/h. Glass samples were either inserted in the furnace at the annealing temperature or heated at 100°C/h from room temperature to the annealing temperature. Crystalline $Na_2Ge_4O_9$, from previous experiments with melts supercooled to 700°C, was annealed at 700°C for 168 h, and was also hydrothermally annealed in a Tuttle-type bomb at 700°C and 2 kbar using a sealed gold capsule in order to contain the mixture of 0.05 g $Na_2Ge_4O_9$ and 0.10 g H_2O.

DISCUSSION

The $A_2Ge_4O_9$-Type Structure of Sodium Tetragermanate

The close correspondence in unit-cell parameters, space group, positional parameters (Table 1), and bond distances and angles (Table 2) between $Na_2Ge_4O_9$ and $K_2Ge_4O_9$ (4) demonstrates unambiguously that $Na_2Ge_4O_9$ does indeed have the $A_2Ge_4O_9$-type structure. All X-ray powder diffraction patterns of $Na_2Ge_4O_9$ presently synthesized were similar, albeit with some variation in the intensities of corresponding reflections, and revealed no evidence for a higher symmetry ($P6_3/m$; derivative wadeite-type) polymorph. Previous assignments of space group $P6_3/m$ (14) and derivative wadeite-type structure for $Na_2Ge_4O_9$ (16) were tenuous. We show below that the wadeite-type structure is unsuitable for $A_2BT_3O_9$ compounds of Na and other medium–large- and medium-sized monovalent cations. Only one very weak reflection in the powder pattern of reference (14), 301 in Table 3, violates the condition limiting possible reflections in space group $P\bar{3}c1$ ($h\bar{h}0l$, $l = 2n$; Miller–Bravais indices). The observed powder pattern from this earlier study otherwise corresponds closely to that calculated using the present structure parameters (Table 3), recognizing that the discrepancies in observed and calculated intensities for 002 and 004 are likely attributable to preferred orientation effects. The derivative wadeite-type structure of reference (16) does not reproduce the observed powder intensities very well, and observed and calculated intensities for three of the reflections used (110, 212, and 312) are in significant disagreement. However, we recognize that the present intersample variation in X-ray powder patterns of $Na_2Ge_4O_9$ may signal transformation behavior in this compound.

Bond distances and angles for GeO_4 tetrahedra and GeO_6 octahedra in the tetrahedral–octahedral framework of $Na_2Ge_4O_9$ are very similar to the corresponding values in $K_2Ge_4O_9$ (Table 2). The essential difference in the two structures is in the accommodation of the smaller (medium–large-sized) Na cation, which is in a $5 + 2$ coordination, with the 5 nearest-neighbor oxygens being in almost square

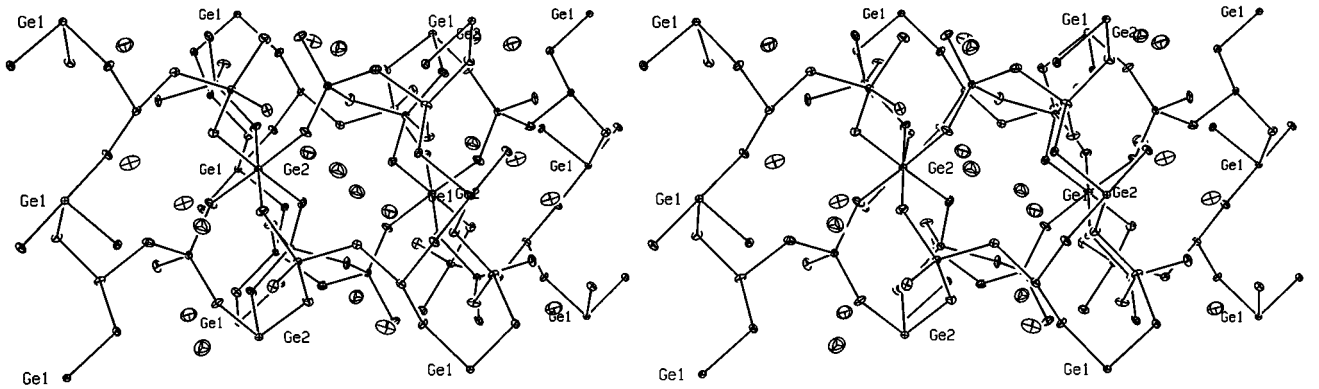

FIG. 2. Stereographic view of structure of sodium tetragermanate ($Na_2Ge_4O_9$), centred at 1/2,1/2,1/2, and showing unit-cell contents. *c*-axis vertical.

pyramidal configuration. The required small displacements of oxygen atoms have been made by crimping the tetrahedral–octahedral framework, i.e., by rotation of GeO_6 octahedra and GeO_4 tetrahedra (Fig. 1), as detailed below. The Ge–O–Ge bond angles in $Na_2Ge_4O_9$ are smaller than in $K_2Ge_4O_9$ by an average of 5.5°.

Alkali Tetragermanate and Tetrasilicate Framework Structures

As noted earlier (2), the factors that are important in tetrahedral (TO_4) framework structures (composition and stoichiometry, T–O bond distance and bond strength, size of large extra-framework cation) are also important in mixed tetrahedral–octahedral framework structures. In particular, accommodation of the large extra-framework cation is of prime importance in determining details of structural topology. The very large monovalent cations (K, Rb, Cs, Ag, and Tl, with effective ionic radii of $^{[8]}$K- 1.51, $^{[8]}$Rb- 1.61, $^{[8]}$Cs- 1.74, $^{[8]}$Ag- 1.28, and $^{[8]}$Tl- 1.59 Å, respectively, for eight-fold coordination with oxygen; 23) prefer cavity positions offering 8 to 12 bonds with oxygen. The Na cation ($^{[8]}$Na- 1.18 Å) is too small for large framework cavities. Usually, the introduction of Na into an aluminosilicate tetrahedral framework results in the distortion of the framework to yield an oval shaped cavity with the Na cation displaced to one end and bonded to fewer oxygens. An additional control limiting mixed tetrahedral–octahedral framework topology in germanates and silicates is the bond valence requirement of oxygens that do not bridge TO_4 tetrahedra (nonbridging oxygens) and are now strongly bonded to a quadrivalent octahedral cation as well as a tetrahedral cation. The single optimum coordination environment for a nonbridging oxygen shared with a $(Ge/Si)O_6$ octahedron, that results in an oxygen bond valence near to 2, is $^{[4]}(Ge/Si) + ^{[6]}(Ge/Si) + 2 \times A$, where A is alkali cation and [4] and [6] refer to tetrahedral and octahedral coordination, respectively.

As noted above, the three known structure types with the formula $A_2B[T_3O_9]$ are wadeite, $A_2Ge_4O_9$, and $Na_2Si_4O_9$. The wadeite-type and $A_2Ge_4O_9$-type structures are both built of $[(Ge/Si)_3O_9]$ three-membered tetrahedral ring units

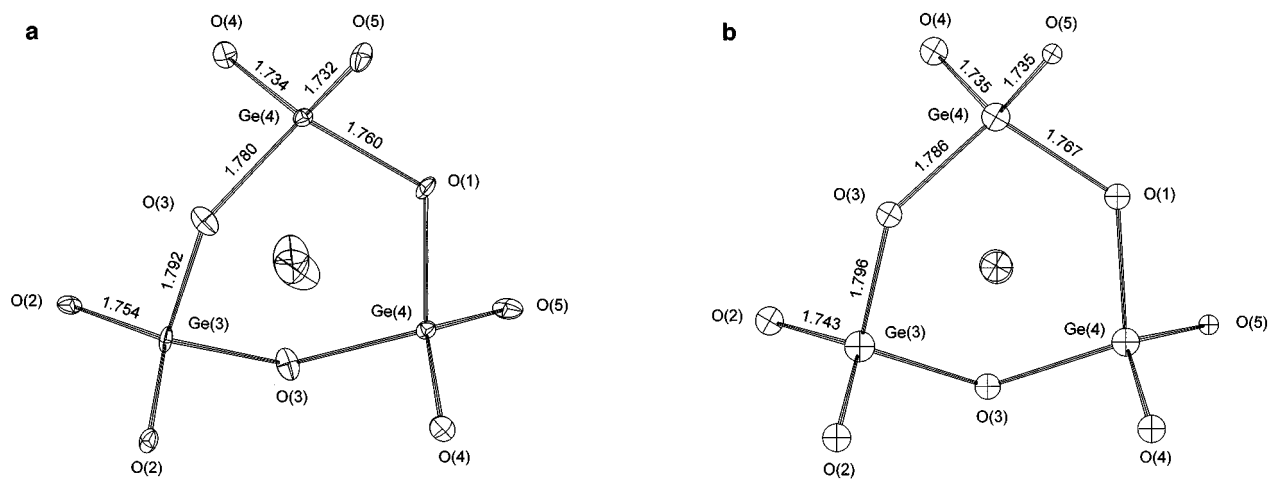

FIG. 3. Geometry of three-membered $[Ge_3O_9]$ ring of GeO_4 tetrahedra in (a) $Na_2Ge_4O_9$ and (b) $K_2Ge_4O_9$ (4). *c*-axis projection, bond distances are Å.

TABLE 1
Positional and Isotropic Thermal Parameters (Å²)
($B_{eq} = \frac{4}{3} \sum_i \sum_j \beta_{ij} a_i \cdot a_j$)

	x	y	z	B_{eq}
Na(1)	0.0074(2)	0.3366(2)	0.4232(2)	1.87(3)
Ge(1)	0.0	0.0	0.0	0.336(10)
Ge(2)	0.33333	0.66667	0.44524(5)	0.394(8)
Ge(3)	0.0	0.17951(4)	0.75	0.478(7)
Ge(4)	0.14937(3)	0.49338(3)	0.70011(3)	0.410(5)
O(1)	0.0	0.4935(3)	0.75	0.67(4)
O(2)	0.0953(2)	0.1542(2)	0.8800(2)	0.56(3)
O(3)	0.1004(2)	0.3245(2)	0.6468(2)	0.77(3)
O(4)	0.2628(2)	0.5125(2)	0.8303(2)	0.70(3)
O(5)	0.1768(2)	0.5921(3)	0.5540(2)	0.74(3)

cross linked by (Ge/Si)O_6 octahedra. In the transverse (c-axis) direction, the octahedra share faces with interspersed unoccupied polyhedra, forming columns (Fig. 4). The principal topological difference between these two structures is the nature of the unoccupied polyhedron. In the wadeite-type structure, alternate octahedra along any column are contrarotated by 180° and the unoccupied polyhedron is a trigonal prism (Fig. 4a). Thus, the three-membered [T_3O_9] ring has nearly ideal geometry, with the Ge cations coplanar with the bridging oxygens and the nonbridging oxygens superimposed parallel to the c-axis. However, in the $A_2Ge_4O_9$-type structure, the unoccupied polyhedron is an octahedron (Fig. 4b). The shared (triangular) octahedral faces, that are cross-linked by the [Ge_3O_9] units, are now contrarotated, causing the [Ge_3O_9] rings to be twisted.

In the high-pressure $K_2Si[Si_3O_9]$ wadeite-type structure (6), K is accommodated in a large cavity position with 3 + 3 + 3 coordination with oxygen, similar to its environment in tridymite-derivative tetrahedral aluminosilicate framework structures. If they existed, wadeite-structure tetragermanates would have an even larger cavity position, because of the longer Ge–O bond distances. In the $A_2Ge_4O_9$-type structure, the twist deformation of the three-membered [Ge_3O_9] ring reduces the size of the framework cavity and adds a degree of freedom to the distortion of the mixed tetrahedral–octahedral framework, permitting a wide range in size of large monovalent cations to be accommodated. In particular, to accommodate the smaller-sized Na cation in $Na_2Ge_4O_9$, the Ge(1)O_6 octahedra, which are on the origin of the unit cell, are contrarotated relative to the $K_2Ge_4O_9$ structure. This displacement rotates the cross-linking Ge(3)O_4 tetrahedron, twisting the three-membered [Ge_3O_9] ring (Fig. 3), and drawing the columns of Ge(1)O_6 octahedra closer together. For alkali tetrasilicates, the [Si_3O_9] tetrahedral ring is too rigid to

TABLE 2
Selected Bond Distances (Å) and Angles (°) for $Na_2Ge_4O_9$ and $K_2Ge_4O_9$

Na–O(1)^{I}		2.584(3)[a]	2.826[b]	Ge(2)–O(5)	×3	1.862(1)[a]	1.883[b]
Na–O(2)^{II}		2.446(2)	2.753	⟨Ge(2)–O⟩		1.870	1.880
Na–O(3)		2.442(2)	2.749	Ge(3)–O(2)	×2	1.754(2)	1.743
Na–O(3)^{III}		2.733(2)	2.734	Ge(3)–O(3)	×2	1.792(2)	1.796
Na–O(4)^{II}		2.615(3)	2.839	⟨Ge(3)–O⟩		1.773	1.769
Na–O(5)		2.847(3)	2.960	Ge(4)–O(1)		1.760(2)	1.767
Na–O(5)^{I}		2.595(3)	2.781	Ge(4)–O(3)		1.780(2)	1.786
⟨Na–O⟩		2.609	2.806	Ge(4)–O(4)		1.734(1)	1.735
Ge(1)–O(2)^{IV}	×6	1.918(2)	1.893	Ge(4)–O(5)		1.732(2)	1.735
⟨Ge(1)–O⟩		1.918	1.893	⟨Ge(4)–O⟩		1.752	1.756
Ge(2)–O(4)^{II}	×3	1.878(2)	1.878				
O(2)–Ge(1)–O(2)^{V}	×6	87.1(1)	88.8[a]	O(1)–Ge(4)–O(3)		107.3(1)	106.7[b]
O(2)–Ge(1)–O(2)^{VI}	×6	92.9(1)	91.2	O(1)–Ge(4)–O(4)		116.9(1)	115.9
O(4)–Ge(2)–O(4)^{VII}	×3	88.5(1)	90.9	O(1)–Ge(4)–O(5)		94.9(1)	94.4
O(4)–Ge(2)–O(5)	×3	89.5(1)	87.9	O(3)–Ge(4)–O(4)		99.1(1)	100.9
O(4)–Ge(2)–O(5)^{V}	×3	90.9(1)	89.7	O(3)–Ge(4)–O(5)		108.4(1)	110.4
O(4)–Ge(2)–O(5)^{VIII}	×3	177.9(1)	178.6	O(4)–Ge(4)–O(5)		129.1(1)	127.5
O(5)–Ge(2)–O(5)^{V}	×3	91.2(1)	91.6	Ge(4)–O(1)–Ge(4)^{IX}		122.4(2)	127.6
O(2)–Ge(3)–O(2)^{IX}		126.8(1)	126.8	Ge(1)^{X}–O(2)–Ge(3)		117.2(1)	124.4
O(2)^{IX}–Ge(3)–O(3)	×2	99.9(1)	103.4	Ge(3)–O(3)–Ge(4)		123.9(1)	126.5
O(2)–Ge(3)–O(3)	×2	112.7(1)	108.2	Ge(2)^{VII}–O(4)–Ge(4)		119.4(1)	127.7
O(3)–Ge(3)–O(3)^{IX}		103.1(1)	105.2	Ge(2)–O(5)–Ge(4)		125.3(1)	129.7

Note. (I) $-x, -y, -z$. (II) $y-x, y, 1/2+x$. (III) $x-y, x, -z$. (IV) $x, y, -1+z$. (V) $-y, x-y, z$. (VI) $y, y-x, -z$. (*VII*) $-y, -x, 1/2+z$. (VIII) $y-x, -x, z$. (IX) $-x, y-x, 1/2-z$. (*X*) $x, y, 1+z$.

[a] $Na_2Ge_4O_9$ (this study).

[b] $K_2Ge_4O_9$ (4).

TABLE 3
Powder X-Ray Diffraction Data for $Na_2Ge_4O_9$ from Reference (14) and Reflection Intensities Calculated with Present Structure (Cu$K\alpha$)

Observed (14)			Calc	Observed (14)			Calc
d_{hkl} (Å)	hkl[a]	I_{rel}	I_{rel}	d_{hkl} (Å)	hkl[a]	I_{rel}	I_{rel}
5.66	110	65	81	2.225	114	5	3
4.89	111	53	56	2.189	321	9	10
4.84	002	44	31	2.172	204	4	3
4.34	102	5	3	2.140	410	6	8
3.68	112	20	14	2.128	223	13	16
3.45	211	20	13	2.080	313	10	8
3.44	202	6	9	2.040	322	10	10
3.26	300	2	1	1.945	304	4	1
3.105	301	1		1.846	323	5	4
2.943	212	35	32	1.818	502	9	5
2.830	220	6	5	1.809	314	5	3
2.802	113	37	27	1.784	413	5	10
2.716	221	59	100	1.759	510	12	20
2.705	302	100	70	1.723	404	5	5
2.442	222	31	31	1.716	215	26	10
2.432	213	33	25	1.635	600	15	28
2.421	004	31	3	1.603	414	9	9
2.370	312	4	3	1.577	315	19	10
2.350	104	24	14	1.570	520	5	5
2.235	320	2	0				

[a] hkl of weaker overlapped reflections and khl of space group $P\bar{3}c1$ not listed.

permit the amount of twist distortion required by the $A_2Ge_4O_9$-type structure, because of the short bond distance and high bond strength of the $^{[4]}$Si–O bond. Hence, high-pressure potassium tetrasilicate adopts the wadeite structure (6), and high-pressure sodium tetrasilicate adopts a framework configuration with a nine-membered $[Si_9O_{27}]$ ring that is collapsed to triclusters of pliable five-membered $^{[4]}$Si–$^{[4]}$Si–$^{[4]}$Si–$^{[4]}$Si–$^{[6]}$Si rings (7).

The size of the framework cavity in mixed tetrahedral–octahedral framework structures varies with the size of tetrahedral and octahedral cations as well as with structural topology. The known structure types for $A_2B[T_3O_9]$ silicates and germanates are summarized in Table 4. From the previous discussion, we might expect the tetrasilicates of Ag, Tl, Rb, and Cs to be stable at high pressure and have the wadeite-type structure. The wadeite-type structure is indeed favored by all of the large- monovalent-cation silicates investigated thus far. The $A_2Ge_4O_9$-type structure is adopted by most alkali metal germanates, but the precise controls on structure type for the largest monovalent cations in the biggest frameworks ($A_2TiGe_3O_9$ and $A_2TiGe_3O_9$) are unclear. The structure types of germanosilicate ($A_2GeSi_3O_9$) and silicogermanate ($A_2SiGe_3O_9$) compounds would clearly be of great interest.

Stability of Sodium Tetragermanate

Sodium tetragermanate and enneagermanate melt congruently at ~1035 and 1073°C, respectively (15). The temperature of the glass transiition (T_g) for the composition $Na_2Ge_4O_9$ is 520°C (24).

Sodium enneagermanate formed in all but one of the present experiments to anneal glass of composition $Na_2Ge_4O_9$, in agreement with references (10, 13, 17), but was not observed to crystallize directly from supercooled melt. Sodium enneagermanate also forms by transformation of sodium tetragermanate, in agreement with reference (10). Our experiments at 700°C are particularly significant since they demonstrate that sodium tetragermanate transforms to the enneagermanate both in air and 2 kbar P(H_2O). On the other hand, sodium tetragermanate consistently formed in melts that were either supercooled to 700°C, in agreement with references (12, 16), or momentarily cooled from 800°C and further annealed at this temperature. Sodium tetragermanate coexisted with sodium enneagermanate, with the tetragermanate dominant, when glass was annealed at 800°C for 2 min, but the enneagermanate appeared alone in a second experiment annealed for 2.5 min. These results confirm that sodium tetragermanate is metastable at all temperatures to the solidus and pressures up to 2 kbar, in agreement with reference (15); the stable assemblage being sodium enneagermanate plus a more sodic phase (e.g., Na_2GeO_3; 17). We speculate that sodium tetragermanate nucleates only in supercooled melts (i.e., above T_g), whereas sodium enneagermanate nucleates from the vitreous state, by transformation of sodium tetragermanates, and from molten salts and aqueous fluids. Crystallization of sodium

TABLE 4
Structure Types of $A_2B[T_3O_9]$ Silicates and Germanates

				B				
A		*T*		Si (0.400)	Ge (0.540)	Ti (0.605)	Sn (0.69)	Zr (0.72)
Na	(1.18)	Si	(0.26)	S(HP)				
		Ge	(0.40)		A			
Ag	(1.28)	Si	(0.26)					
		Ge	(0.40)		A			
K	(1.46)	Si	(0.26)	W(HP)		W	W	W
		Ge	(0.40)		A	A	A	
Tl	(1.59)	Si	(0.26)					
		Ge	(0.40)			W	A	
Rb	(1.60)	Si	(0.26)			W	W	
		Ge	(0.40)		A	A	A	
Cs	(1.74)	Si	(0.26)					
		Ge	(0.40)			W	W	

Note. Effective ionic radii (in parentheses; Å) from Ref. (23). Structure types: S—$Na_2Si_4O_9$; W—wadeite; A—$A_2Ge_4O_9$. HP is high pressure.

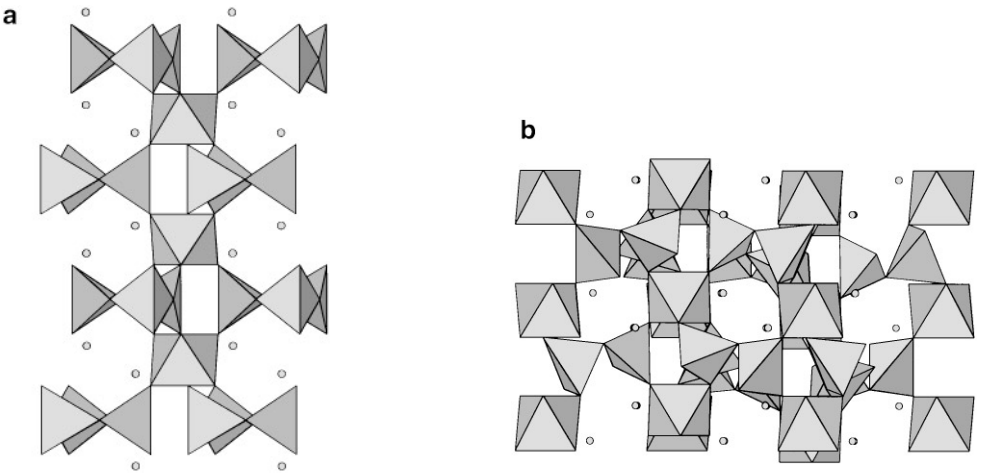

FIG. 4. Relationship of three-membered $[Ge_3O_9]$ ring unit to the GeO_6 octahedron in (a) wadeite-type structure, [010] projection, showing *c*-axis column formed from the GeO_6 octahedron and interspersed unoccupied trigonal prism that results in a near-ideal ring geometry, and (b) $A_2Ge_4O_9$-type structure of $Na_2Ge_4O_9$, [120] projection, showing *c*-axis column formed from the GeO_6 octahedron and interspersed unoccupied octahedron that results in a twisted ring geometry.

enneagermanate by very slow cooling of melts in air to 600–700°C (12, 16) is consistent with this reconstruction, since in this procedure sodium enneagermanate likely forms by transformation of preexisting sodium tetragermanate.

The pressure stabilities of sodium tetragermanate and enneagermanate have not been extensively investigated and may be of interest because the tetragermanate is the denser phase; e.g., $D_x = 4.45$ and 4.24 g cm^{-3}, respectively. This is surprising, since the enneagermanate has greater proportions of both GeO_2 and octahedral Ge; the ratio of $^{[6]}$Ge : $^{[4]}$Ge being 1 : 3 in the tetragermanate and 4 : 5 in the enneagermanate. Evidently, the spiral $[Ge_4O_{12}]_n$ chain contributes significant low-packing density to the enneagermanate structure. However, this spiral chain is likely to be relatively compressible. Thus, sodium enneagermanate could well persist in preference to sodium tetragermanate at pressures greatly in excess of the 2 kbar limit presently investigated.

ACKNOWLEDGMENTS

We thank Y. Thibeau for assistance with X-ray powder diffraction and the Natural Sciences and Engineering Research Council of Canada for financial support.

REFERENCES

1. L. W. Finger and R. M. Hazen, *Acta Crystallogr. Sect. B* **47,** 561 (1991).
2. M. E. Fleet and G. S. Henderson, *Phys. Chem. Mineral.* **24,** 345 (1997).
3. D.E. Henshaw, *Mineral. Mag.* **30,** 585 (1955).
4. H. Völlenkle and A. Wittmann, *Monatsh. Chem.* **102,** 1245 (1971).
5. J. Choisnet, A. Deschanvres, and B. Raveau, *J. Solid State Chem.* **7,** 408 (1973).
6. D. K. Swanson and C. T. Prewitt, *Am. Mineral.* **68,** 581 (1983).
7. M. E. Fleet, *Am. Mineral.* **81,** 1105 (1996).
8. A. Wittmann and E. Modern, *Monatsh. Chem.* **96,** 581 (1965).
9. H. Völlenkle, A. Wittmann, and H. Nowotny, *Monatsh. Chem.* **100,** 79 (1969).
10. H. Nowotny and A. Wittmann, *Monatsh. Chem.* **85,** 558 (1954).
11. J. F. White, E. R. Shaw, J. F. Corwin, and A. Pabst, *Anal. Chem.* **31,** 315 (1959).
12. A. Wittmann and P. Papamantellos, *Monatsh. Chem.* **91,** 855 (1960).
13. M. K. Murthy and J. Aguayo, *J. Am. Ceram. Soc.* **47,** 444 (1964).
14. J. H. Jolly and R.L. Myklebust, *Acta Crystallogr. Sect. B* **24,** 460 (1968).
15. B. Monnaye and R. Bouaziz, *C. R. Acad. Sci. Ser. C* **271,** 1581 (1970).
16. S. Sakka, K. Kamiya, and T. Mizuno, "Res. Rept. Fac. Eng., Mie Univ., Japan," pp. 73–86, 1977.
17. C. I. Ajuwa, A. Mayer, and W. Zednicek, *J. Mater. Sci. Lett.* **12,** 1214 (1993).
18. G. Eulenberger, A. Wittmann, and H. Nowotny, *Monatsh. Chem.* **93,** 123 (1962).
19. N. Ingri and G. Lundgren, *Acta Chem. Scand.* **17,** 617 (1963).
20. M. E. Fleet, *Acta Crystallogr. Sect. C* **46,** 1202 (1990).
21. E. R. Shaw, J. F. Corwin, and J.W. Edwards, *J. Am. Chem. Soc.* **80,** 1536 (1958).
22. J. A. Ibers and W. C. Hamilton (Eds.), "International Tables for X-Ray Crystallography," Vol. IV. Kynoch Press, Birmingham, UK, 1974.
23. R. D. Shannon, *Acta Crystallogr. Sect. A* **32,** 751 (1976).
24. O. V. Mazurin, M. V. Streltsina, and T. P. Shvaiko-Shvaikovskaya, "Handbook of Glass Data," Part B. Elsevier, Amsterdam, 1985.